

# Activated drift motion of a classical particle with a dynamical pinning effect

F. Thalmann<sup>a</sup>

LEPES-CNRS, BP 166X, 25 avenue des Martyrs, 38042 Grenoble Cedex, France

Received: 12 December 1997 / Accepted: 25 February 1998

**Abstract.** A one dimensional trap model for a thermally activated classical particle is introduced to simulate driven dynamics in presence of “ageing” effects. The depth of each trap increases with the time elapsed since the particle has fallen into it. The consequences of this dynamical pinning are studied, and velocity-force characteristics are numerically obtained. A special attention is paid to the situation where the particle is pulled with a spring to ensure a finite average velocity. In the low velocity regime, the presence of a broad distribution of trapping times leads to suppression of linear response, replaced by a threshold or by sublinear dynamics. A regime of strong fluctuations is obtained when the particle is driven at intermediate velocities.

**PACS.** 05.40.+j Fluctuation phenomena, random processes, and Brownian motion

## 1 Introduction

The out-of-equilibrium dynamics of glassy systems is a widely open subject. An important topic concerns models for which a spontaneous ageing behavior competes with an external field. This article aims to study a realization of the above paradigm in a simple “friction” experiment where the two main features – ageing and external forcing – are present. For this purpose, a stochastic process describing a classical particle in a one-dimensional pinning potential is defined. The pinning potential consists of identical traps with time-dependent depths. The barriers between two neighbouring traps therefore increase with time in order to simulate ageing effects, and the hopping rate between traps is based on Arrhenius dynamics. Some physical justifications for such time-dependent barriers are exposed in Section 2. Indeed, by choosing adequately the time dependence of the trapping potential, one can account for anomalous slow diffusion situations related to broad algebraic distributions of waiting times and leading to glassy behaviors [1,2]. One can alternatively consider a simpler case where the barriers increase from a short-time value to a larger long-time value and discuss the related dynamical consequences.

Our main purpose is to understand the driven dynamics of this system in the situation where the average velocity  $v$  is non zero. A quadratic potential moving at velocity  $v$  is therefore added, acting in a way similar to a spring pulling a body in a friction experiment. The mean spring extension defines the friction force  $F$ . The relation between  $v$  and  $F$  is called the “Velocity-Force”

characteristics, and is the central output for such a friction experiment. Other quantities of interest will be monitored like the distribution of waiting times between hops or the histogram of the “spring lengths”. In some situations, the time-dependent pinning potential is found to enhance the fluctuations of the particle position.

The basic feature of this model consists in a competition between the “ageing” pinning coming from the traps, and the renewal due to the driven dynamics. It results in a strongly non-linear  $v - F$  characteristics for a wide intermediate velocity regime. The more extreme case of logarithmic growing barriers leads to a non-ohmic behaviour at low velocity, typical of glassy systems. In the latter case, a naive, “mean-field like”, regularization with a characteristic interruption time  $t_c(v)$ , fails in describing the low-velocity properties of the model. The limit  $v \rightarrow 0$  indeed appears to be singular and involves large pinning times  $\sim 1/v$ .

Section 2 provides physical justifications of the model, detailed in Section 3. A physical application is discussed. Section 4 focuses on the velocity-force characteristics induced by logarithmic growing barriers. Then, Section 5 studies some consequences of rapidly growing barriers on the particle’s dynamics.

## 2 A review of mechanisms generating an effective time dependent pinning potential

### 2.1 A time dependent pinning potential

Many disordered systems like spin glasses, pinned random manifolds, diffusing particles in random media, involve a

---

<sup>a</sup> e-mail: thalmann@lepes.polycnrs-gre.fr

disordered energy landscape. In such systems, thermal effects, – diffusion and activation – compete against pinning effects. At low enough temperature, the out-of-equilibrium dynamics is usually governed by activated barrier crossings in the configuration space. When the distribution of energy barriers is broad, the time scale for reaching a thermal – Boltzmann – equilibrium may diverge with the size of the system.

By following a particle during its out-of-equilibrium dynamics, one can attempt to define a function of time, with dimension of an energy, as the mean (or typical) height of the barrier that the system has to overcome, in order to expand further. This function “ $\mathcal{H}(t)$ ” will be the starting point for this phenomenological approach of driven dynamics.

For instance, many aspects of the slow thermal diffusion of a particle in a one-dimensional quenched random force field, first introduced by Sinai, have been partially reinterpreted as the consequence of such effective barriers, slowly increasing with time [1]. The random force generates a pinning potential – in 1 dimension – with unbound local extrema, and the particle has to overcome higher and higher barriers in trying to reach its thermal equilibrium. Let  $t_w$  be the time interval elapsed since the beginning of the diffusion process, or waiting time. After  $t_w$ , the particle is shown to be at equilibrium within a restricted area bounded by a barrier of height  $\mathcal{H}(t_w) \sim T \ln(t_w)$  [1, 3]. Such a growing effective barrier induces a strong dependence in  $t_w$ , or ageing, for the response and diffusion properties of the particle, together with an “anomalous” slow diffusion behavior. A generalization to other types of correlated disorder potentials leads to a variety of interesting regimes with sublinear characteristics [4, 5].

In a related way, the ageing properties of a particle diffusing in a high dimensional phase space within traps with exponentially distributed depths, were extensively studied, in relation with the magnetic relaxation of spin glasses [2]. Again, after a waiting time  $t_w$ , the particle stays in a trap of typical depth  $\mathcal{H}(t_w) \sim T \ln(t_w)$  [8]. Such a situation may occur for instance when describing the creep of an extended object like an elastic manifold. The pinning energy of this object increases as its internal degrees of freedom wander and find favorable configurations. One expects that the longer the object stays at the same place, the larger its pinning energy will be. A well known example involving pinning and motion of elastic lines concerns the flux line problem in high  $T_c$  superconductors [9].

However, we must keep in mind that many other systems have slow relaxation properties which do not originate from a barrier pinning mechanism. This is the case for a particle evolving in a high dimensional, random pinning potential [6]. In this system, thermal activated processes cannot explain the whole dynamics, because a non trivial relaxation subsists when the temperature goes to 0. In such situations, the slow dynamics is attributed to “entropic effects”, *i.e.* the system has more and more difficulties to find favorable regions in its phase space, even if it is not separated from them by any energy barrier

[7]. The existence of growing effective energy barriers is therefore only a sufficient condition for ageing.

In what follows, Section 4 deals with particles diffusing among traps whose depth increases like  $T \ln(t_w)$ , leading to a power law distribution for waiting times. In the last Section 5, we focus on a less singular case where the time-dependent barrier  $\mathcal{H}(\infty) < \infty$  does not diverge.

## 2.2 Detail of the friction experiment

In a friction experiment, one can either impose the external driving force  $\mathbf{F}$  or the velocity drift  $\mathbf{v}$ . In the first case,  $\mathbf{F}$  is a constant and one measures the mean position  $\langle x(t) \rangle$  of the particle. One can alternatively pull the particle with a spring, with the other end moving at constant velocity  $v$ . By doing so, one enforces only the average velocity, and the force is then related to the mean extension of the spring.

Some systems make these two procedures be inequivalent. Some examples of random walks over random traps which exhibits only a sub-linear response for the mean displacement  $\langle x(t) \rangle \propto t^\alpha$ ;  $\alpha < 1$  are reviewed in [10]. On the contrary, driving the particle with a spring ensures that the average displacement  $x(t)$  is linear in time, in other words the average velocity always exists, provided the average is taken on sufficiently long times. Nevertheless, anomalous diffusion effects are still present and appears through the effective friction force, with the disappearance of the usual linear regime at low velocity. The study of such thermal “creep” for traps models generalized in a way to allow the particle to be driven by a spring, will be the main purpose of Section 4. As far as possible, results for the spring driven case will be compared to their “constant force” counterparts.

On physical grounds, besides its “regularization” effect, the quadratic confinement potential may reflect more complicated systems. For instance, when describing a set of interacting particles, a crude mean-field elastic approximation produces a “cage potential” (self-averaging contribution of the whole system) which limits the excursion of a given particle [16]. This potential moves at velocity  $v$  with the center of gravity of the entire body. It can therefore be considered as a first step towards the incorporation of interactions in anomalous diffusion problems.

As far as real “dry” friction experiments are concerned, it is known that phenomena similar to ageing occur at the contacts, and should be responsible for both the slow time dependence of threshold forces and for the “stick-slip” motion [11, 12]. Spring pulling and velocity dependent ageing are already present in reference [11] but their model is designed for a very different purpose. First, they introduce a very strong ageing leading to a reentrant velocity-force characteristics and unstable motion. Then, they consider only a crude “mean-field” approach, called “adiabatic approximation”.

In what follows we focus on overdamped, thermally activated motion, and especially on the low-velocity creep motion. In contrast with the model of reference [11], the

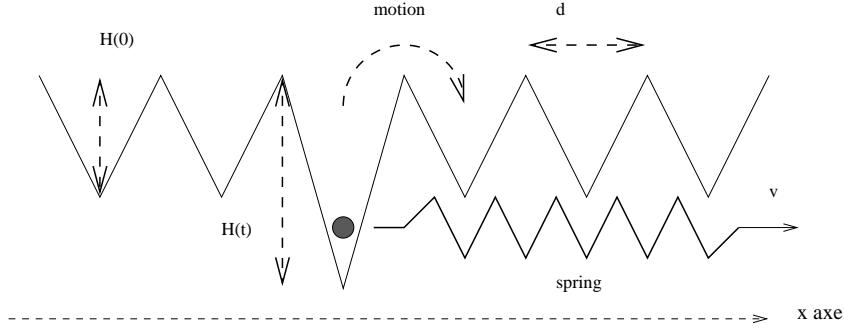


**Fig. 1.** Schematic illustration of the friction experiment.

ageing process is here described through a broad distribution of trapping times, and the dynamics is simulated, giving access to nonlinear creep characteristics as well as to fluctuation effects. We provide details on the stochastic process and consider carefully the whole distribution of waiting times and spring lengths, which turn out to have a crucial importance for understanding the physical contents of this model: the dangers of a naive mean-field approach are emphasized in Section 4.

### 3 Trap dynamics in presence of an external driving force

We consider a saw-tooth potential made of equidistant triangular wells (Fig. 1). The interval between two sites is constant, equal to  $d$ . The particle is supposed to hop towards its nearest neighbours sites, at a rate given by the Arrhenius law. Whereas the conventional “reaction rate theory” requires additional information about the specific shape of the barrier, and provides corrective terms [13], we will keep only the crude Arrhenius ratio. When a particle falls into a well, this one starts to increase its depth, in order to mimic an effective barrier  $\mathcal{H}(t)$  growing with time. The corresponding escape rate decreases accordingly, generating longer waiting times. A particle escaping from a well, immediately falls into one of its nearest neighbours. The particle is then always trapped, excepted during the negligible transit delay over the barrier. The saw-tooth potential is quite arbitrary, and the Arrhenius dynamics insensitive to this specific shape.

An external potential – constant driving force or spring traction – tilts the saw-tooth potential, reduces one of the two barriers and increases the instantaneous escape rate. The barrier is strongly reduced by any external bias, until it vanishes at the critical force  $F_c(t) = 2\mathcal{H}(t)/d$ . Let  $h^-(\tau)$  and  $h^+(\tau)$  be the height of the left and right barrier (Fig. 2).  $\tau$  is the time elapsed since the arrival of the particle in the occupied trap. By adding the left and right “channels”, the total escape rate  $w_{tot}$  reads, ( $\beta$  standing for the inverse temperature  $T^{-1}$ ,  $\omega_0$  for a trial frequency):

$$w_{tot}(\tau) = \frac{\omega_0}{2} \exp(-\beta h^+(\tau)) + \frac{\omega_0}{2} \exp(-\beta h^-(\tau)). \quad (1)$$

In absence of external force, the left and right barriers coincide and are set equal to  $\mathcal{H}(t)$ . By choosing  $\mathcal{H}(t)$  ar-

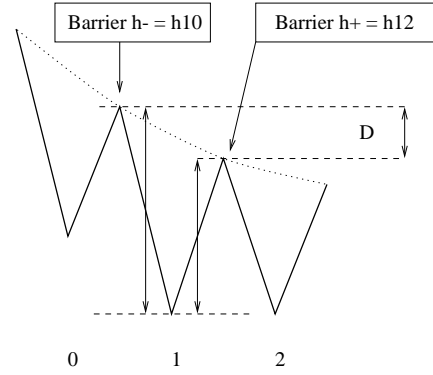


**Fig. 2.** Barriers  $h^-$  and  $h^+$  (Sect. 3).

bitrarily, one can generate all the possible waiting time distributions.  $\mathcal{H}$  constant corresponds to an ordinary activated diffusion over identical traps, leading to a diffusion constant  $D$  and mobility  $\mu$ :

$$D = \frac{\omega_0 d^2}{2} \exp(-\beta \mathcal{H}), \quad \mu = \frac{\beta \omega_0 d^2}{2} \exp(-\beta \mathcal{H}). \quad (2)$$

An external force  $F$  changes  $\mathcal{H} \rightarrow \{h^+ = \mathcal{H} - Fd/2; h^- = \mathcal{H} + Fd/2\}$ , leading to the constant force  $F$  escape rate:

$$w_{tot}(\tau) = \omega_0 \exp(-\beta \mathcal{H}(\tau)) \operatorname{ch} \left( \frac{\beta F d}{2} \right). \quad (3)$$

A spring of stiffness  $k$ , with a head moving at constant velocity  $v$  and the particle located at  $x(t)$  exerts a force  $F(t) = kl(t)$  with  $l(t) = vt - x(t)$ . The total escape rate  $w_{tot}(\tau, l_{(\tau=0)})$  reads:

$$\omega_1 \exp[-\beta \mathcal{H}(\tau) + \beta \mathcal{H}(0)] \operatorname{ch} \left( \frac{\beta k d (v t - x(t))}{2} \right), \quad (4)$$

$$\omega_1 = \left\{ \omega_0 \exp \left( -\frac{\beta k d^2}{8} \right) \exp(-\beta \mathcal{H}(0)) \right\}.$$

It's essential to distinguish between the total time  $t$  and the delay  $\tau$  relative to the more recent jump of the particle, which occurred at  $t - \tau$ . Once the value of  $l_{(\tau=0)}$  is known, at the time of arrival of the particle, (4) determines the

probability distribution for the waiting time before the next jump.

As expected, the external force affects the escape rate. At large times, the hyperbolic cosine dominates the exponential term and make the particle eventually depin. Depinning is fast when  $w_{tot}$  becomes larger than 1, which happens when the force is greater than the critical ratio  $2\mathcal{H}(\tau)/d$ .

Let's denote by  $\Pi(t)$  the probability for the particle to stay within the well for a time  $\tau$  longer than  $t$ .  $\Pi(t)$  decays exponentially as:

$$\Pi(t) = \exp\left(-\int_0^t ds w_{tot}(s, l_{(s=0)})\right). \quad (5)$$

By definition,  $\pi(t) = -d\Pi(t)/dt$  is the probability distribution of waiting times. The knowledge of  $\Pi(t)$  allows to perform ‘‘molecular dynamics’’ simulations by following a procedure close to BKL [14]. In this simulation scheme, one computes at each step, the waiting time  $\tau$  before the next jump. This is achieved by converting a uniform random number  $r \in [0, 1]$  into  $\tau(r)$ , *i.e.* by inverting  $\Pi(\tau) = r$ .

The stochastic process consists in a sequence of jumps, labeled by  $i$ . Each jump has a random direction  $\sigma_i = \pm 1$  (left or right), and a random waiting time  $\tau_i \in [0, \infty[$ . The total time  $t_n$ , particle position  $x_n$ , and the spring extension  $l_n$  follow the recurrence equations:

$$\begin{cases} t_n = t_{n-1} + \tau_n \\ x_n = x_{n-1} + \sigma_n d \\ l_n = l_{n-1} - \sigma_n d + v\tau_n. \end{cases} \quad (6)$$

A fundamental difference distinguishes constant force and spring friction experiments. In the first case, the waiting times  $\tau_i$  are statistically independent, while in the second case, they are strongly correlated, because their probability distribution is conditioned by the spring extension  $l(t)$ , which varies slowly. For example, a long waiting time extends the spring, and forces the next waiting times to be shorter than the average. These correlations prevent from performing a complete analytical study, and justify a numerical approach. By defining  $V = (\beta k d v)/2$ ,  $X(t) = (\beta k d x(t))/2$ ,  $L(t) = X(t) - Vt$ ,  $\Delta = (\beta k d^2)/2$ , the cosine term becomes  $\text{ch}(Vt + L(t))$ . A spring length  $L(t) \sim 1$  means that the external force has reached its critical value  $F_c \simeq 2\mathcal{H}/d$ .  $L(t)$  is piece-wise linear, increasing during the pinning of the particle, and with discontinuities  $-\sigma_i \Delta$  at each jump. A small value of  $\Delta$  means that the particle has many different traps accessible. At the opposite, for  $\Delta \geq 1$ , the spring forces the particle to occupy only one given site or its nearest neighbours. This regime has not been considered here.

Provided the temperature is not too low,  $\omega_0^{-1}$ ,  $\omega_1^{-1}$ , and the characteristic time for the effective barrier are of the same order and constitute a unique, microscopic, time scale. We have restricted ourselves to this situation ( $\beta \sim 1$ ). The only independent parameters of the model turn to be: those defining  $\mathcal{H}$ , the rescaled jump length  $\Delta$  and the ‘‘velocity’’  $V\omega_1^{-1}$ .

The mean friction force is given by

$$\langle F \rangle = \frac{2T}{d} \langle L(t) \rangle, \quad (7)$$

where brackets stand for the time average.

$\langle O \rangle = \lim_{\Theta \rightarrow \infty} \frac{1}{\Theta} \int_0^\Theta O(s) ds$ . The exact formulas for the mean position  $L$  and its quadratic fluctuation  $L^2$  are:

$$\begin{aligned} \langle L \rangle &= \lim_{n \rightarrow \infty} \frac{\sum_{i=1}^n L(t_i) \tau_i + V \tau_i^2 / 2}{\sum_{i=1}^n \tau_i} \\ \langle L^2 \rangle &= \lim_{n \rightarrow \infty} \frac{\sum_{i=1}^n L(t_i)^2 \tau_i + L(t_i) V \tau_i^2 + V^2 \tau_i^3 / 3}{\sum_{i=1}^n \tau_i} \end{aligned}$$

There is no need to average over a quenched disorder in this model, and simulations are notably simplified. We stress however that the time averages mentioned above may present important fluctuations from one realization of the process to another. This is especially the case when a broad distribution of trapping time is considered, and the displacement  $x(t)$  as a function of time may exhibit fluctuations as large as  $\langle x(t) \rangle$  itself. Note that our numerical work corresponds to spring pulling experiments, thus trapping time distributions are regularized. We have checked carefully that the time averages were well defined and converged.

At each jump, the direction  $\sigma_n = 1$  is chosen with probability  $p(\tau_n, t_{n-1})$  and  $\sigma_n = -1$  with probability  $1 - p$ . We made the choice

$$\begin{aligned} p(\tau_n, t_{n-1}) &= \frac{\exp(-\beta h^+(\tau_n))}{\exp(-\beta h^+(\tau_n)) + \exp(-\beta h^-(\tau_n))} \\ &= \frac{1}{1 + \exp[-2L(t_{n-1}) - 2V\tau_n]}. \end{aligned} \quad (8)$$

Restricted to the case  $V = 0$  and  $\mathcal{H}$  constant, the above choice fulfills the detailed balance equation, and the resulting Boltzmann equilibrium distribution for  $l(t)$  is a Gaussian with variance  $T/k$ .

One can demonstrate that the general case  $V = 0$ , but  $\mathcal{H}$  increasing, still leads to a stationary distribution profile for  $l(t)$ , provided the mean trapping time exists, *i.e.*  $\mathcal{H}$  must be a bounded or slowly increasing function of time.

## 4 Large algebraic waiting time distributions

### 4.1 Definitions

It is well known that ageing effects appear when the waiting time distribution decays like  $\pi(\tau) \sim \tau^{-(1+\alpha)}$  and  $\alpha < 1$ . The following choice ( $\tau_1 = 1/\omega_1$  is the reference time scale):

$$\Pi(t) = \left(1 + \frac{\tau}{\alpha \tau_1}\right)^{-\alpha}, \quad \pi(t) = \frac{1}{\tau_1} \left(1 + \frac{\tau}{\alpha \tau_1}\right)^{-(\alpha+1)}, \quad (9)$$

is obtained, following (5), with

$$\beta\mathcal{H}(\tau) = \ln\left(1 + \frac{\tau}{\alpha\tau_1}\right), \text{ and} \quad (10)$$

$$w_{tot}(\tau) = \frac{\alpha}{\alpha\tau_1 + \tau}. \quad (11)$$

When a constant force  $F$  is applied, one has:

$$w_{tot}(\tau) = \left(\frac{\alpha}{\alpha\tau_1 + \tau}\right) \text{ch}(\beta Fd/2). \quad (12)$$

The effective exponent is no longer  $\alpha$ , but  $\alpha'(F) = \alpha \text{ch}(\beta Fd/2)$  and the hopping length  $d$  remains constant. This picture is different from the one emerging from the Sinai model, where the force dependent exponent is  $\alpha(F) = F/F_c$  ( $F_c$  is a given critical force), and the typical hopping length depends on  $F$  like  $d(F) \sim 1/F^2$ . This latter phenomenology could be used as another starting point instead of equations (3, 4, 6).

The behaviour of a system with  $\mathcal{H}$  growing as above, and a weak constant force  $F$  is just a particular case of the ‘‘continuous time random walks’’ described in [10]. The mean displacement  $\langle x(t) \rangle$  of the particle turns out to be in this case (disregarding prefactors):

$$\langle x(t) \rangle = N(t)dt \left(\frac{Fd}{2T}\right) \quad (13)$$

$$\langle x(t) \rangle \simeq \frac{d^2}{2T} \left(\frac{t}{\tau_1}\right)^\alpha F, \quad (14)$$

$N(t)$  is the typical number of jumps during the time interval  $[0, t]$ , and functions of  $\beta Fd/2$  have been linearized in the last equation. The sublinear dependence in time means that the velocity is asymptotically 0.

Let us turn now to the system with a spring pulling the particle at constant velocity  $v$ . The constant force result (14) is helpless in this case. This is precisely a situation where driving with a spring is inequivalent to driving with a constant force. In this case, the broad waiting time distribution is cut when the spring depins the particle. A cut-off time  $t_c$  is defined as:

$$kl(t_c) = kv t_c = F_c = \frac{\mathcal{H}(t_c)}{d/2}, \quad (15)$$

$$\frac{t_c}{\ln(1 + t_c/\alpha\tau_1)} = \frac{2}{k\beta d} \frac{1}{v}. \quad (16)$$

## 4.2 A mean field approach

One can try to understand the creep behaviour of the system by a mean field argument, by neglecting all the fluctuations in the force and writing  $F = k \langle l(t) \rangle$ . Owing to the regularization provided by the velocity, the mean value of the waiting times exists and equals:

$$\langle \tau(v) \rangle = \tau_1 \left(\frac{t_c(v)}{\tau_1}\right)^{1-\alpha}. \quad (17)$$

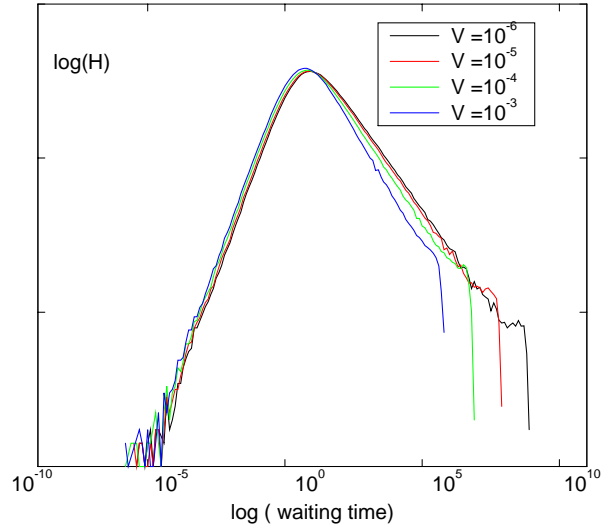


**Fig. 3.** Distribution of waiting times regularized by the velocity. ( $\alpha = 0.5$ ). This curve  $H(\ln t)$  has to be understood as follows: the number of waiting times lying between  $t_1$  and  $t_2$  is  $N(t_1, t_2) = \mathcal{N} \int_{t_1}^{t_2} H(\ln t) d \ln t$ . ( $\mathcal{N}$  is a normalization factor).  $H(\ln t) \sim t^{-\alpha}$ .

Result (13) holds, and one can write a self-consistent equation for  $v$ ,  $v \ll 1$ .

$$vt = F \frac{d^2}{2T} \frac{1}{t_c(v)} \left(\frac{t_c(v)}{\tau_1}\right)^\alpha t, \quad (18)$$

which, apart from a logarithmic factor, leads to  $t_c(v) \sim 1/v$  and:

$$F = \frac{2\tau_1}{\beta d^2} \left(\frac{2}{\beta k d \tau_1}\right)^{1-\alpha} v^\alpha. \quad (19)$$

The linearized case  $\beta Fd/2 \leq 1$  implies  $\alpha' = \alpha \text{ch}(\beta Fd/2) \simeq \alpha$  (at weak velocity, the force does not change much the value of  $\alpha'$ ). This mean field approach gives a power law creep  $F \sim v^\alpha$ . Unfortunately, it strongly disagrees with numerical simulations.

The simulations were done, following the scheme of equation (6), Section 2. Details on the computational scheme are deferred to the Appendix: the main difficulty comes from the conversion of random numbers in waiting times, and a trick is necessary to avoid computer time wasting.

## 4.3 Analysis of the numerical results

Figure 3 shows an histogram for the distribution of waiting times with  $\alpha = 0.5$ , at various velocities. The distributions are clearly cut at  $t_c(v)$ . The constant slope  $-(1 + \alpha')$  in the log-log plot shows that one has true power laws until the cut-off. At intermediate velocities,  $\alpha'$  departs from its 0 velocity value, as expected.

Figure 4 shows the dependence of the  $v - F$  curve in the exponent  $\alpha$ . The characteristics have been found

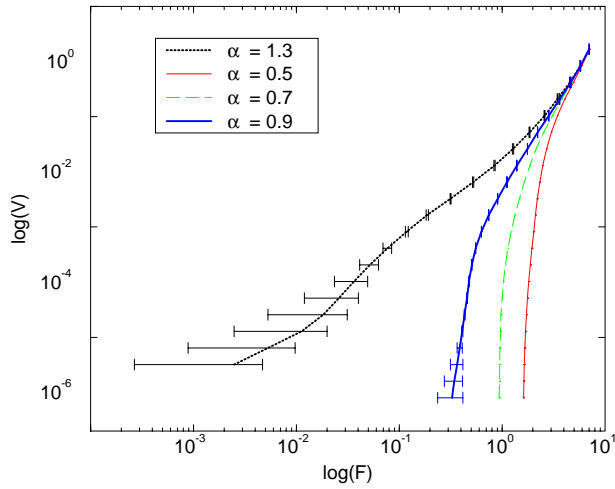


**Fig. 4.** Dependence of the  $v - F$  curve in the exponent  $\alpha$ . The closer to 1 is  $\alpha$ , the more difficult is the convergence at low velocities.  $\Delta = 0.005$ ;  $V = 0.5\beta kd$  ranges from  $4 \times 10^{-8}$  to 0.1.

to be monotonic and increasing. For both  $\alpha = 0.9$  and  $\alpha = 1.3$ , the curves are presented with horizontal error bars (which are very small for  $\alpha = 0.5$  and  $\alpha = 0.7$ ). They give an estimate for the fluctuations between successive runs. The convergence is all the more difficult to get that the velocity is weak and the exponent  $\alpha$  close to 1. All the characteristics with  $\alpha < 1$  have a threshold value decreasing while  $\alpha$  becomes closer to 1. For  $\alpha > 1$ , one should recover an ohmic regime at low velocities. The characteristics for  $\alpha = 1.3$  are compatible with such an ohmic response, but fluctuations from one run to another remain important. This is probably a consequence of the infinite mean squared value of the waiting times when  $v \rightarrow 0$

In log-log coordinates, the  $v - F$  curves are concave, and seems at first glance to end at a threshold value  $F(v \rightarrow 0)$  whereas in linear coordinates, at the opposite, they are convex. Among the curves known to change their convexity when the axes are logarithmically graduated, one finds for example the celebrated stretched exponentials  $v = v_0 \exp[-(f_c/f)^\gamma]$  occurring in some glassy creep cases [9]. For  $\alpha = 0.5$  such a functional form fits well the intermediate regime  $10^{-4} < v < 10^{-1}$  with  $\gamma \sim 2.8 \pm 0.1$ , but does not describe anymore the slower regime  $v < 10^{-4}$ . This latter case is better fitted by a threshold characteristics  $F_c + (F - F_c)^\beta$ ,  $\beta = 2.1$  (over only 1 decade).

One can roughly say that the  $v - F$  curve, for  $\alpha = 0.5$ , has a threshold value  $F_c$  with a force  $F$  which does not vary by more than 12% over 2 decades. This is enough to discard the mean field description mentioned above (Eq. (19)). The other values of  $\alpha = 0.7; 0.9$  exhibits a similar threshold force, but as  $\alpha$  becomes closer to 1, it is more and more difficult to get a good, well converged value for the force at weak velocity and the fit with the stretched exponential becomes poor.

One can account for the existence of the quasi-threshold behaviour of the  $v - F$  curve (*i.e.* up to loga-

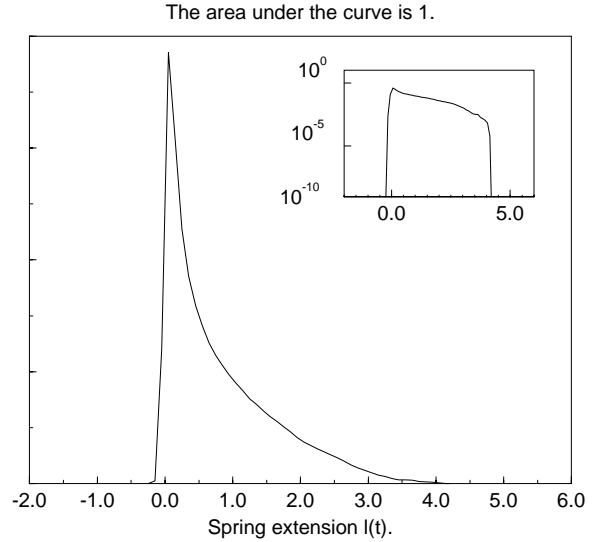


**Fig. 5.** The histogram of spring lengths  $L(t) (= \beta kd l(t)/2)$  does not center around 0, even for a vanishing velocity (here  $v = 10^{-6}$ ). The inset shows the histogram with a logarithmic vertical axe.

rithmic factors) with a simple argument. The distribution of waiting times is a broad power law distribution cut for times greater than  $\sim d/v$ . The contribution of large waiting times  $\tau \sim d/v$  represents a finite ratio of the total sum  $t = \sum_{i=1}^n \tau_i$ . Such waiting times correspond to a finite value for the spring extension  $kv\tau$ , and occur at a constant rate. As they are not balanced by any negative contribution, the resulting mean spring extension remains finite. Figure 5 confirms this scenario. The histogram for the variable  $l_i$  remains asymmetric, even for a vanishing velocity, leading to a constant friction force. The “mean-field” approach fails because it relies on the existence of a typical value  $F$  for the force, vanishing with  $v$ , in contradiction with Figure 5.

It is interesting to notice that the mean-field procedure leads to a (wrong) power law creep at low velocity. Such power laws have been found by Horner in the mean-field theory of a particle in a short range correlated disorder [15]. Whereas it is a rather different problem, where ageing comes from slow relaxation in a high dimensional phase space, and not from any barrier mechanism (Sect. 2.1), we emphasize that both mean-field approaches lead to a power law for  $v \rightarrow 0$ . One can suspect the corrective terms to the above mean-field theory (which contain all thermal activation effects) to modify the algebraic creep into a threshold, like here.

Anyway, in every physical case, it must exist a huge but finite equilibration time  $t_{eq}$ , at which the effective barrier  $\mathcal{H}$  stops increasing. The above threshold characteristics must match with a slow thermally activated ohmic regime for velocities  $v \leq d/t_{eq}$ .

## 5 Velocity induced fluctuations

### 5.1 A stepwise potential

The necessary and sufficient condition for the existence of an ohmic regime at low velocity is that the mean trapping time  $\langle\tau\rangle$  remains finite. This is because the effective “viscosity”  $\eta = \lim_{v \rightarrow 0} F/v$  scales like  $\langle\tau\rangle$ . At the opposite,  $\langle\tau\rangle = \infty$  implies a sublinear or “creep” regime in the  $v - F$  characteristics. This latter can always be written:

$$F = \eta v, \quad (20)$$

where  $\eta$  depends on  $F$  or on  $v$  according to the friction experiment considered. When using a time-dependent potential  $\mathcal{H}$ , one can generate a distribution of waiting times strongly dependent on  $v$ , with consequently, a non constant mean pinning time  $\langle\tau(v)\rangle$ , decreasing with  $v$ .

Whenever  $\mathcal{H}$  remains bounded, one expects a crossover between the strong velocity regime involving  $\mathcal{H}(\tau \simeq 0)$  and the low velocity regime depending on the whole range  $\tau \in [0, \infty[$ . Moreover, a detailed study of the fluctuations  $\langle l^2(t) \rangle$  of the particle’s position turns out to be very instructive and reveals some unexpected features.

In order to make apparent the effects of a non-constant  $\mathcal{H}$  function, I have introduced a decreasing step function. Such a sharp behaviour for  $\mathcal{H}$  should make the crossover well contrasted. This is done with the escape rate:

$$w_{tot}^0 = \begin{cases} \omega_1 & \text{for } \tau \in [0, t_s] \\ \omega_2 & \text{for } \tau \in [t_s, \infty[ \end{cases}, \quad (21)$$

where  $t_s$  is the arbitrary position of the step. The  $\Pi(t)$  function (5) and its reciprocal  $\Pi^{-1}$  can be computed exactly, providing an easy numerical generation of waiting times.  $\Pi(t)$  equals:

$$\begin{aligned} t < t_s: & \exp \left[ \frac{\omega_1}{V} (\text{sh}(L) - \text{sh}(L + Vt)) \right], \\ t > t_s: & \exp \left[ \frac{\omega_1}{V} \text{sh}(L) + \frac{\omega_2 - \omega_1}{V} \text{sh}(L + Vt_s) \right. \\ & \left. - \frac{\omega_2}{V} \text{sh}(L + Vt) \right]. \end{aligned} \quad (22)$$

### 5.2 The enhancement of fluctuations

The mean square value is computed and compared with the equilibrium one, given by the energy equipartition theorem  $k \langle l^2(t) \rangle = T$ , where  $k$  denotes the spring stiffness.

In Figure 6 the ratio  $\varphi = k \langle l^2(t) \rangle / T$  is plotted for the special choices  $\omega_1 = 1$ ,  $\omega_2 = 0.01 (= 1\% \omega_1)$ ,  $t_s$  ranging from 0.5 to 7. The results are compared with the constant  $\mathcal{H}$  cases A:  $w_{tot}^0 = \omega_1$  and B:  $w_{tot}^0 = \omega_2$ . The step function case S interpolates between these two static pinning potential cases. Thus, one expects the results for S to fall in between the two extreme cases A and B.

The  $v - F$  characteristics behaves in this way (see Fig. 7). Whereas the constant  $w_{tot}^0$  cases A and B exhibits

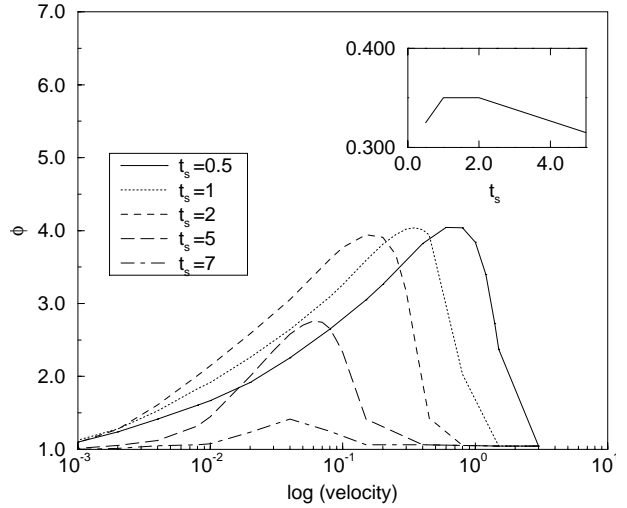


**Fig. 6.**  $\phi = k\beta \langle l^2(t) \rangle$  ratio between fluctuations and equilibrium fluctuations. The stepwise  $\mathcal{H}$  cases S lead to a maximum at  $v = v_{max}$ . The constant  $\mathcal{H}$  cases A, B are characterized by  $\phi \simeq 1$  (not on this picture). The inset shows the product  $v_{max}t_s$  vs.  $t_s$ , which has a constant value  $\sim 0.33$ .

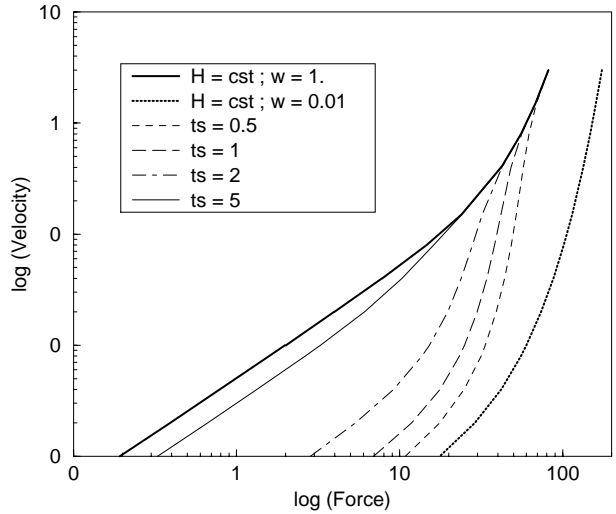


**Fig. 7.** Comparison of the velocity force characteristics, between the constant  $w$  cases A and B, and the stepwise  $w$  cases S. The time  $t_s$  of the step ranges from 0.5 to 5.

fluctuations very close to equilibrium ones, regardless to the value  $\omega$ , the stepwise situation S shows a maximum for an intermediate regime centered around  $t_s^{-1}$ . Fluctuations are enhanced with a factor 3 or 4, before reaching their near equilibrium value at high velocities (Fig. 6).

The value  $\varphi \simeq 1$  at high velocities suggests a decoupling between translation motion and fluctuations, similar to the one due to the galilean invariance, in the disorderless case. This is reminiscent from a well known result about a fast particle moving on a random potential. When considering a particle driven at high velocity, with a force greater than the critical one, the pinning potential plays only a perturbative role. The random pinning force acts

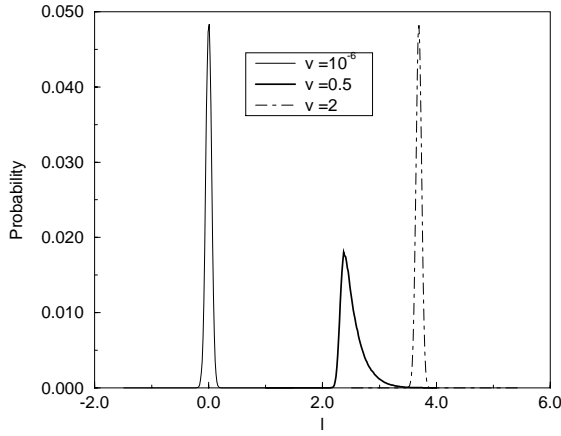


**Fig. 8.** The distribution of spring lengths  $L(t)$  is a Gaussian at low and high velocities and is stretched at intermediate velocities.

like a Langevin noise and leads to an effective “shaking temperature” scaling like the inverse velocity  $1/v$  (as far as a single particle is considered) [17].

The effect of fluctuations is thus maximal at intermediate velocities. In the context of a friction experiment, such anomalous fluctuations are reminiscent of “stick-slip” phenomena. On the other hand, in the physical case where the spring potential mimics the elastic interactions between particles, a strong fluctuation regime indicates that the motion occurs with strong deformations, with a possible breakdown of the elastic regime towards a plastic one. At the opposite, at weak or large velocities, the motion of the particles may be coherent, within an homogeneous flow [17] (two neighbouring particles remain close for a long time). The onset of such a “plastic flow” should occur when the amount of fluctuations  $\langle x^2 \rangle$  reaches a critical value like in the celebrated Lindemann criterion for melting.

Figure 8 shows histograms for weak  $v = 10^{-5}$ , intermediate  $v = 0.5$  and high velocity  $v = 2$ . The step occurs at  $t_s = 1$ .  $\varphi \simeq 1$  corresponds to a Gaussian shape of the  $l(t)$  distribution,  $\varphi > 1$  coincides with an asymmetric distribution for  $l(t)$ , with a tail on the right, related to large values of  $l$ . The presence of such strong fluctuations requires a high enough velocity, able to “convert” a long pinning time into a large value of  $l$ . At the other extreme, if  $v$  is too large, the friction force is higher than the critical force, and the pinning is no more efficient. The effect is maximal for  $0.32 < vt_s < 0.35$ .

## 6 Conclusion

In this paper, a general stochastic process has been defined, which allows dynamical pinning effects, by introducing time-dependent barriers. The model has first been specialized to generate power-law distributed waiting times. The case of a particle driven by a spring has been investigated and compared to the previously known constant

driving force case. The sublinear drift of the latter case is found to have a counterpart which in the present study appears as a finite threshold for the friction force, even for vanishing velocities. A naive mean-field approach fails in describing the velocity-force characteristics, showing the prominent role of large waiting times, even within a distribution cut-off by the drift motion. The analogy with the  $D = \infty$  “mean field” result suggests that the finite dimension corrections could drive the power-law creep into a threshold characteristics, ultimately linear at very low velocities if the distribution of waiting times is cut by size effects.

Then, we have investigated the consequences of a time dependent pinning potential concerning the fluctuations in the particle position. It has been achieved with a sharp step profile for the time dependent barrier. Fluctuations are strongly enhanced at an intermediate velocity regime. This phenomenon is important in various physical cases where the simple model presented here applies and deserves more investigations.

More generally, this model provides a general framework in order to test the equivalence between applied force and applied velocity in a friction experiment, with presence of “surface ageing” and at a scale where the temperature is a relevant parameter.

I thank J.P Bouchaud, A.Valat, J. Farago, J-L. Gilson and D. Feinberg for fruitful discussions, and D. Feinberg especially for a critical reading of the manuscript. I am indebted to W. Krauth for his lecture about Monte-Carlo methods at Beg Rohu Summer School of Physics (France) 1996.

## Appendix: Random generation of waiting times

Given a random number  $r$  taken from a uniform distribution over  $[0, 1]$ , the corresponding waiting time  $\tau$  is  $\Pi^{-1}(r)$ , with  $\Pi^{-1}(\Pi(s)) = s$  and  $\Pi$  defined by (5). As the integration cannot be – in the general case – performed analytically, a direct evaluation of  $\tau$  requires to find numerically the root of a function defined by a quadrature. Independently, convergence requires many millions ( $10^7$  to  $10^8$ ) numbers  $\tau_i$  at low velocities, excluding any direct computation scheme for  $\Pi^{-1}$ .

It’s natural to look for asymptotic approximations of the integral. First, one notices that the integrand  $w_{tot}^0(\tau) \text{ch}(Vt+L)$  has at least two very different time scales  $\omega_1^{-1}$  and  $V^{-1}$ .

Let us detail the particular case  $\alpha \text{ch}(Vt+L)/(\alpha\tau_1 + t)$ . On the one hand, if  $Vt \ll 1$ , the integral becomes  $\text{ch}(L) \int_0^t \alpha ds / (\alpha\tau_1 + s)$ , leading to:

$$\tau(r) = \alpha\tau_1 \left[ \exp\left(-\frac{\ln(r)}{\alpha \text{ch}(L)}\right) - 1 \right]. \quad (23)$$

On the other hand,  $Vt \geq 1$  describes situations where the force  $kl(t)$  approaches the critical depinning value.



It's very unlikely to find high value  $L \gg 1$  or negative  $L \ll -1$ . In order to cover the range  $Vt \simeq 1$ ,  $\Pi^{-1}$  has been tabulated, by a direct numerical calculation, for a grid in the plane  $(L, \ln V)$  with variable  $L$  between  $-3 < L < 5$ ;  $\Delta L = 0.1$  and variable  $V$ ,  $10^{-8} < V < 1$  with 20 values following a geometrical sequence. At each point of the grid  $\Pi^{-1}(r)$  is approximated with a Tchebitchev polynomials approximation, by keeping the 30 first coefficients.

When a couple  $(L, \ln V)$  not on the grid is required, its Tchebitchev coefficients are linearly interpolated. The conversion  $\tau(r)$  is reduced to a fast polynomial evaluation.

The two previous approximations match fine for  $Vt \simeq 0.01$ , and were actually used in the simulation.

## References

1. M. Feigel'man, V. Vinokur, J. Phys. I France **49**, 1731 (1988).
2. J.P. Bouchaud, J. Phys. I France **2**, 1705 (1992).
3. R. Maynard, J. Phys. Lett. France **45**, L81 (1984).
4. S. Scheidl, Z. Phys. B **97**, 345 (1995).
5. P. Le Doussal, V. Vinokur, Physica C **254**, 63 (1995).
6. S. Franz, M. Mézard, Europhys. Lett. **26**, 209 (1994); L. Cugliandolo, P. Le Doussal, Phys. Rev. E **53**, 1525 (1996).
7. See for example J. Kurchan, L. Laloux, J. Phys. A **29**, 1929 (1996); F. Ritort, Phys. Rev. Lett **75**, 1190 (1995); A. Barrat, M. Mézard, J. Phys. I France **5**, 941 (1995).
8. By adjusting the distribution of the successive barriers that a particle, in a one dimensional case, has to overcome, L. Laloux and P. Le Doussal are able to reproduce almost all the possible ageing behaviors, cond-mat/9705249.
9. G. Blatter, *et al.*, Rev. Mod. Phys. **66**, 1125 (1994).
10. J.P. Bouchaud, A. Georges, Phys. Rep. **195**, 127 (1987).
11. F. Heslot, *et al.*, Phys. Rev. E **49**, 4973 (1994).
12. C. Caroli, P. Nozières, in *Physics of Sliding Friction* (Kluwer Academic, Dordrecht, 1996).
13. P. Hänggi, P. Talkner, M. Borkovec, Rev. Mod. Phys. **62**, 251 (1990).
14. A. Bortz, M. Kalos, J. Lebowitz, J. Comput. Phys **17**, 10 (1975).
15. H. Horner, Z. Phys. B **100**, 243 (1996).
16. D. Fisher, Phys. Rev. Lett. **50**, 1486 (1983). For the depinning of Charge Density Waves.
17. For a review of velocity induced phase transitions in the context of high Tc superconductors see A. Koshelev, V. Vinokur, Phys. Rev. Lett **73**, 3580 (1994); T. Giamarchi, P. Le Doussal, preprint cond-mat/9708085, (1996).